Crystal Growth, Crystal Structure, and Magnetic Properties of a New Lithium Cobalt Diphosphate

F. Sanz,[†] C. Parada,[‡] and C. Ruiz-Valero*,[†]

Instituto de Ciencia de Materiales de Madrid, CSIC, Cantoblanco, E−28049 Madrid, Spain, and Departamento de Química Inorgánica, Facultad de Ciencias Químicas, Universidad Complutense, E−28040 Madrid, Spain

Received June 25, 1999. Revised Manuscript Received December 15, 1999

Single crystals of the new lithium cobalt diphosphate $Li_6Co_5(P_2O_7)_4$ have been grown, and their structure has been determined by X-ray diffraction techniques. This compound crystallizes in the triclinic space group $P\bar{1}$ with $a = 6.3009(7)$, $b = 8.413(1)$, and $c = 9.937(1)$ Å, $\alpha = 107.894(2)$, $\beta = 90.247(2)$, and $\gamma = 92.782(2)°$, $V = 500.6(1)$ Å^3, and $Z = 1$. The structure of $Li_6Co_5(P_2O_7)_4$ is characterized by the arrangement of CoO_6 octahedra, CoO_5 trigonal bipyramids, and diphosphate groups. The CoO_6 octahedra share edges forming infinite zigzag chains $[Co_3O_{14}]$ running along the *b* direction. Laterally, such chains share octahedra corners with CoO_5 trigonal bipyramids and P_2O_7 diphosphate groups connecting with another symmetrically equivalent chain. The connection between these polyhedra defines tunnels along the [100], [001], and [011] directions, where the Li cations are located. The tunnel intersection gives rise to a three-dimensional channel system. Magnetic measurements reveal the presence of antiferromagnetic interactions in the Co^{2+} sublattice at about 11 K. The field dependence of magnetization shows that this compound exhibits a metamagnetic transition.

Introduction

The phosphates of transition metals form a wide family of compounds showing many interesting properties.[1] For this reason, a great effort, has been devoted to the study of mixed transition-metal phosphates during the past years. However, few investigations on the structure of diphosphates containing Li and transition metal are reported in the literature. There exist complete structural data only for $LiM(P_2O_7)$ (M = Mo,[2] Fe,[3] V[4]), $Li_2Cu(P_2O_7)$,[5] $Li_2Pd(P_2O_7)$,[6] $LiMoO(P_2O_7)$,[7] and $LiNi_{1.5}P_2O_7$.[8]

In this paper, which is an extension of our work on mixed phosphates[9−11] containing alkaline and transition-metal cations, we present the synthesis, crystal structure determination, and magnetic properties of the new lithium cobalt diphosphate $Li_6Co_5(P_2O_7)_4$. We are interested in the role the alkali metal environment may play in affecting the crystal structure of these phosphates and consequently its influence in their properties.

Experimental Section

Synthesis. Crystals of $Li_6Co_5(P_2O_7)_4$ were grown by melting a mixture of $Li_4P_2O_7$ and $Co_2P_2O_7$ in the molar ratio Li/Co = 6:5. Because $Li_4P_2O_7$ and $Co_2P_2O_7$ are not commercially available reactants, they were previously synthesized. $Li_4P_2O_7$ was obtained as was reported in a previous work.[12] $Co_2P_2O_7$ was obtained from $CoCO_3{\cdot}4H_2O$ and $NH_4H_2PO_4$ in the molar ratio Co/P = 1:1. These reactants were well-mixed in an agate mortar and heated to 300 °C. Later, the mixture was reground and heated to 600 °C for 1 day. After these treatments, the X-ray diffraction pattern of the well-crystallized solid corresponds to that of $Co_2P_2O_7$ (Powder Diffraction File No. 39-0709).

The mixture of $Li_4P_2O_7$ and $Co_2P_2O_7$ was slowly heated to 700 °C in a porcelain crucible. The furnace was kept at this temperature for 2 h to homogenize the melt; then, it was cooled at 10 °C/h to 400 °C and finally quenched to room temperature. Many violet crystals with prismatic form were extracted from the resulting product, which yields the composition $Li_6Co_5(P_2O_7)_4$, as deduced from the structure determination.

The new phase $Li_6Co_5(P_2O_7)_4$ was also obtained as a microcrystalline powder by solid-state reaction employing as precursors $Li_4P_2O_7$ and $Co_2P_2O_7$ in the molar ratio Li/Co = 6:5, which were well-mixed and ground in an agate mortar. An accumulative thermal treatment was performed at 300, 400, 500, 600, and 650 °C for 24 h at each temperature. The well-

* To whom correspondence should be addressed. E-mail: caridad@immrx1.icmm.csic.es. Telephone:+34 91 3349026. Fax:+34 91 3720623.
† CSIC.
‡ Universidad Complutense.

(1) Borel, M. M.; Goreaud, M.; Grandin, A.; Labbé, Ph.; Leclair, A.; Raveau, B. *Eur. J. Solid State Inorg. Chem.* **1991**, *23*, 93.
(2) Wang, S. L.; Wang, P. C.; Nieh, Y. P. *J. Appl. Crystallogr.* **1990**, *23*, 520.
(3) Riou, D.; Nguyen, N.; Benloucif, R.; Raveau, B. *Mater. Res. Bull.* **1990**, *25*, 1363.
(4) Lii, K. H.; Wang Y. P.; Chen, Y. B.; Wang, S. L. *J. Solid State Chem.* **1990**, *86*, 143.
(5) Spirlet, M. R.; Rebizant, J.; Liegeois-Duyckaerts, M. *Acta Crystallogr.* **1993**, *C49*, 209.
(6) Laligant, Y. *Eur. J. Solid State Inorg. Chem.* **1992**, *29*, 239.
(7) Ledain, S.; Borel, M. M.; Leclaire, A.; Provost, J.; Raveau, B. *J. Solid State Chem.* **1995**, *120*, 260.
(8) Rissouli, K.; Benkjouja, K.; Sadel, A.; Bettach, M.; Zahir, M.; Giorgi Pierrot, M. *Acta Crystallogr.* **1996**, *C52*, 2960.
(9) Sanz, F.; Parada, C.; Amador, U.; Monge, M. A.; Ruiz-Valero, C. *J. Solid State Chem.* **1996**, *123*, 129.
(10) Sanz, F.; Parada, C.; Ruiz-Valero, C. *J. Solid State Chem.* **1999**, *145*, 604−611.
(11) Sanz, F.; Parada, C.; Rojo, J. M.; Ruiz-Valero, C.; Saez-Puche, R. *Chem. Mater.* **1999**, *11*, 2673−2679.
(12) Tien, T. Y.; Hummel, F. A. *J. Am. Ceram. Soc.* **1961**, *44*, 206.

10.1021/cm991085+ CCC: $19.00
Published on Web 02/12/2000

Table 1. Crystal Data and Structure Refinement for $Li_6Co_5(P_2O_7)_4$

empirical formula	$Li_{5.88}Co_{5.06}P_8O_{28}$
formula weight	1038.99
temperature	295 (2) K
wavelength	0.71073
crystal system	triclinic
space group	$P\bar{1}$
unit cell dimensions	$a = 6.3009(7)$ Å, $\alpha = 107.894\ (2)°$ $b = 8.413\ (1)$ Å, $\beta = 90.247\ (2)°$ $c = 9.937\ (1)$ Å, $\gamma = 92.782\ (2)°$
volume, Z	500.6 (1) Å^3, 1
density (calcd)	3.446 Mg/m^3
absorption coefficient	4.845 mm^{-1}
$F(000)$	497
crystal size	0.08 × 0.04 × 0.04 mm^3
θ range for data collection	2.15−23.29°
limiting indices	(−6,−9,−9) (6,9,11)
reflections collected	2150
independent reflections	1408 ($R_{int} = 0.0295$)
refinement method	full-matrix least-squares on F^2
data/ restraints/parameters	1408/0/199
goodness-of-fit on F^2	1.049
final R indices [$I > 2\sigma(I)$]	$R_1 = 0.0460$, $wR_2 = 0.1229$
R indices (all data)	$R_1 = 0.0488$, $wR_2 = 0.1260$
extinction coefficient	0.046 (5)
largest diff. peak and hole	2.648 and −1.139 eÅ^{-3}

crystallized violet powder at the end of the process was a single phase because the X-ray powder diffraction pattern of the bulk product compared well with that calculated from single-crystal data.

Elemental Analysis. Chemical analyses of selected single crystals were carried out on an ICP (inductively coupled plasma) apparatus. The calculated and experimental molar ratios Li/Co/P are 3.9/28.8/23.9 and (4.0 ± 0.4)/(29.0 ± 0.2)/(24.2 ± 0.3), respectively.

Single Crystal X-ray Diffraction. A summary of the conditions for data collection is given in Table 1. A violet crystal of prismatic shape was resin epoxy-coated and mounted on a Siemens Smart CCD diffractometer equipped with a normal focus, 2.4 kW sealed-tube X-ray source (Mo Kα radiation, $\lambda = 0.71073$ Å) operating at 50 kV and 40 mA. Data were collected over a hemisphere of reciprocal space by a combination of three sets of exposures. Each set had a different φ angle for the crystal, and each 20 s exposure covered 0.3° in ω. The crystal-to-detector distance was 6.01 cm. Coverage of the unique set was over 99% complete to at least 23° in θ. Unit cell dimensions were determined by a least-squares fit of 40 reflections with $I > 20\sigma(I)$ and $4° < 2\theta < 46°$. The first 30 frames of data were recollected at the end of the data collection to monitor crystal decay. The intensities were corrected for Lorentz and polarization effects. Scattering factors for neutral atoms and anomalous dispersion corrections for Co and P were taken from the *International Tables for Crystallography*.[13] The structure was solved by Patterson methods and refined in the triclinic space group $P\bar{1}$. Full-matrix least-squares refinement with anisotropic thermal parameters for Co, P, and O, and isotropic for Li atoms was carried out by minimizing $w(F_0^2 - F_c^2)$.[2] After a very small or even a negative temperature factor was obtained for Li(4), the occupancy factor of this atom was refined with a fixed thermal parameter that was the average of the other Li atoms. After several cycles of refinement. this factor rose to 2.01(2). This electron density corresponds to 6e$^-$, given that there is no other atom involved in the synthesis procedure (confirmed by the elemental analysis), the only possibility to generate this electron density would be the existence of some Co impurity sharing this position. This shared position has been observed before in other transition-metal phosphates.[14,15] When the isotropic temperature factor and the population factor were refined together for this shared position (Li,Co)(4), they reached 0.878(5) and 0.122(5) for Li and Co occupation, respectively, and the temperature factor was slightly higher than the average for Li atoms, and these values remained unchanged. Three crystals showing well-defined faces were fully analyzed, giving identical refinements (position and site occupancy for Li(4)). To maintain the electrical neutrality a 6% Co vacancy is assumed, and the obtained composition is $Li_{5.88}Co_{5.06}(P_2O_7)_4$. It is worthwhile to point out the small difference between the R value of 0.046 for observed reflections with $I > 2\sigma(I)$, and that of 0.049 for all reflections, which indicates the goodness of the model for the weak reflections, too. Refinement on F^2 for all reflections, weighted R factors (R_w), and all goodness of fit S are based on F^2, whereas conventional R factors (R) are based on F; R factors based on F^2 are statistically about twice as large as those based on F, and R factors based on all data will be even larger.

All calculations were performed using SMART software for data collection, SAINT[16] for data reduction, SHELXTL™ [17] to resolve and refine the structure and to prepare material for publication, and ATOMS[18] for molecular graphics.

X-ray Powder Diffraction. The X-ray powder diffraction pattern was taken at room temperature by using a Siemens D-500 diffractometer in the step scan mode, Cu Kα (λ = 1.540 598 Å) radiation, at a step value of 0.02°, measuring for 20 s at each step. The observed reflections were indexed on a triclinic unit cell using the TREOR program[19] in a very good agreement with the parameters obtained from the single-crystal X-ray study.

Magnetic Measurements. Magnetic susceptibility was measured using a Quantum Design MPMS-XL SQUID magnetometer operating from 300 to 2 K at 1000 Oe.

Results and Discussion

Crystal Structure. A summary of the fundamental crystal data for $Li_6Co_5(P_2O_7)_4$ is given in Table 1. Final atomic coordinates and selected bond distances and angles are given in Tables 2 and 3, respectively.

The structure of $Li_6Co_5(P_2O_7)_4$ is characterized by the arrangement of CoO_6 octahedra, CoO_5 trigonal bipyramids, and P_2O_7 diphosphate groups.

There are three crystallographically independent cobalt atoms. Co(1) and Co(2) are octahedrally coordinated, and Co(3) exhibits trigonal bipyramid coordination with averages Co−O distances of 2.092(5), 2.117(5), and 2.066(5) Å for Co(1), Co(2), and Co(3), respectively. The Co(1) and Co(2) octahedra share edges in such a way that they are mutually independent and form chains which run parallel to the b axis, the sequence in the chain being Co(2)−Co(1)−Co(2), Figure 1. The Co(1) atom is situated in an inversion center at the (1b) position. According to this symmetry, Co(1) is between two Co(2) octahedra sharing the O(6)−O(13)′ edge with one Co(2), and the O(6)′−O(13) edge with the other Co(2). Every two $Co(2)O_6$ octahedra share the O(8)−O(8)′ edge, giving a zigzag arrangement. There is no connection among $Co(3)O_5$ polyhedra, because each of them is connected to one $Co(2)O_6$ octahedron through a

(13) *International Tables for Crystallography*; Kynoch Press: Birmingham, U.K., 1974; Vol. 4, p 72.
(14) Angenault, J.; Couturier, J.; Quarton, M. *Eur. J. Solid State Inorg. Chem.* **1995**, *32*, 335.
(15) Dridi, N.; Boukhari, A.; Réau, J. M.; Holt, E. M. *Solid State Ionics* **1998**, *107*, 25.
(16) Siemens. *SAINT*, data collection and procedure software for the SMART system; Siemens Analitical X-ray Instruments, Inc.; Madison, WI, 1995.
(17) Siemens. *SHELXTL*, ver 5.0; Siemens Analitical X-ray Instruments, Inc.; Madison, WI, 1995.
(18) Dowty, E. *ATOMS* for Windows 3.1, a computer program for displaying atomic structure; Kingsport, TN, 1995.
(19) Werner, P. E. University of Stockholm s-106, 91, Stockholm, Sweden, 1984.

Table 2. Atomic Coordinates and Equivalent Isotropic Displacement Parameters [Å² × 10³] for $Li_6Co_5(P_2O_7)_4$

atom	*x*	*y*	*z*	$U_{(eq)}$[a]
Co(1)	0.5000	0.5000	0.0000	9(1)
Co(2)	−0.3549(2)	0.1194(1)	−0.0588(1)	9(1)
Co(3)	−0.6895(2)	−0.1106(1)	−0.3546(1)	11(1)
P(1)	0.5236(3)	0.2465(2)	−0.3197(2)	8(1)
P(2)	0.1523(3)	0.2057(2)	0.0161(2)	8(1)
P(3)	0.2637(3)	0.5407(2)	−0.2623(2)	9(1)
P(4)	0.1867(3)	0.1813(2)	−0.6894(2)	9(1)
Li(1)	−0.980(3)	0.162(2)	−0.389(2)	34(4)
Li(2)	0.5000	0.5000	−0.5000	23(4)
Li(3)	−0.089(3)	0.395(2)	−0.123(2)	36(4)
Li,Co(4)[b]	0.0000	0.5000	−0.5000	43(5)
O(1)	0.2371(8)	0.3535(6)	−0.5905(5)	15(1)
O(2)	0.4587(8)	0.4233(6)	−0.3315(5)	9(1)
O(3)	0.2237(8)	0.3841(6)	0.0274(6)	14(1)
O(4)	−0.0426(9)	0.1594(6)	−0.0793(5)	12(1)
O(5)	−0.3850(8)	−0.0811(6)	−0.2615(5)	10(1)
O(6)	0.3954(8)	0.7096(6)	0.1665(5)	11(1)
O(7)	−1.0185(8)	−0.0858(6)	−0.3685(5)	12(1)
O(8)	−0.6742(8)	0.0793(6)	−0.0311(5)	11(1)
O(9)	−0.6735(8)	0.1321(6)	−0.3487(6)	14(1)
O(10)	0.0692(8)	0.4260(6)	−0.2774(6)	15(1)
O(11)	−0.6996(8)	−0.1947(6)	−0.5759(5)	13(1)
O(12)	−0.0805(8)	−0.2017(6)	−0.1685(5)	12(1)
O(13)	0.3350(8)	0.6332(6)	−0.1127(5)	13(1)
O(14)	−0.7404(8)	−0.3507(6)	−0.3594(5)	10(1)

[a] *U*(eq) is defined as one-third of the trace of the orthogonal $\mathbf{U}_{ij}$ tensor. [b] Li,Co(4) sites are randomly occupied by 0.878(5) Li, and 0.122(5) Co.

common O(5) oxygen atom and the other four vertexes are shared with diphosphate groups.

The two diphosphate anions are built from two different PO_4 phosphate tetrahedra. The PO_4 polyhedra are far from being regular. The distortion observed could be explained on the bases of steric considerations and the electrostatic repulsion between electronic clouds.[20] The longest bonds in the PO_4 tetrahedra are always found along P−O−P bridges. Among the six terminal

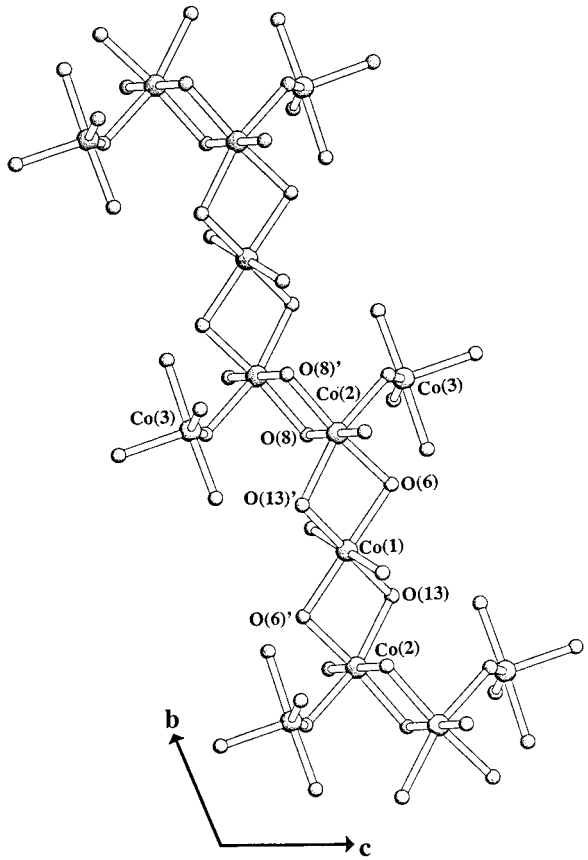

Figure 1. Metal chains in $Li_6Co_5(P_2O_7)_4$ occurring throughout −Co(3)Co(2)O_9−Co(2)Co(3)O_9−Co(1)O_6 sequences.

P−O bonds of each diphosphate group, the nearest oxygens, which may or may not be weakly connected to Co atoms, are O(1) and O(10). Both are apical oxygens

Table 3. Selected Bond Lengths (Å) and Angles (deg) for $Li_6Co_5(P_2O_7)_4$

Co(1)−O(3)	×2	2.015(5)	Li(1)−O(7[c])		2.29(2)
Co(1)−O(6)	×2	2.147(5)	Li(1)−O(9)		2.03(2)
Co(1)−O(13)	×2	2.113(5)	Li(1)−O(10[d])		2.16(2)
Co(2)−O(4)		2.002(5)	Li(1)−O(11[c])		2.08(2)
Co(2)−O(5)		2.195(5)	Li(2)−O(1)	×2	2.044(5)
Co(2)−O(8)		2.058(5)	Li(2)−O(2)	×2	1.985(5)
Co(2)−O(6[a])		2.065(5)	Li(2)−O(14[e])	×2	2.225(5)
Co(2)−O(8[b])		2.138(5)	Li(3)−O(3)		2.49(2)
Co(2)−O(13[a])		2.246(5)	Li(3)−O(3[a])		2.04(2)
Co(3)−O(5)		2.097(5)	Li(3)−O(4)		2.19(2)
Co(3)−O(7)		2.102(5)	Li(3)−O(6[a])		2.07(2)
Co(3)−O(9)		2.022(5)	Li(3)−O(10)		1.91(2)
Co(3)−O(11)		2.093(5)	Li,Co(4)−O(1)	×2	2.017(5)
Co(3)−O(14)		2.015(5)	Li,Co(4)−O(10)	×2	2.517(5)
Li(1)−O(7)		2.16(2)	Li,Co(4)−O(14[e])	×2	2.216(5)
O(3[f])−Co(1)−O(3)		180.0	O(8)−Co(2)−O(13[a])		93.2(2)
O(3)−Co(1)−O(13)	×2	89.7(2)	O(6[a])−Co(2)−O(5)		88.7(2)
O(3)−Co(1)−O(13[f])	×2	90.3(2)	O(4)−Co(2)−O(13[a])		85.7(2)
O(3)−Co(1)−O(6)	×2	85.3(2)	O(6[a])−Co(2)−O(13[a])		76.4(2)
O(13)−Co(1)−O(6)	×2	77.6(2)	O(5)−Co(2)−O(13[a])		165.1(2)
O(3)−Co(1)−O(6[f])	×2	94.7(2)	O(14)−Co(3)−O(11)		87.8(2)
O(13[f])−Co(1)−O(6)	×2	102.4(2)	O(14)−Co(3)−O(7)		90.5(2)
O(6[f])−Co(1)−O(6)		180.0	O(11)−Co(3)−O(7)		86.0(2)
O(13[f])−Co(1)−O(13)		180.0	O(9)−Co(3)−O(5)		90.3(2)
O(4)−Co(2)−O(6[a])		86.1(2)	O(7)−Co(3)−O(5)		158.1(2)
O(4)−Co(2)−O(8[b])		95.8(2)	O(14)−Co(3)−O(9)		173.7(2)
O(6[a])−Co(2)−O(8[b])		173.4(2)	O(9)−Co(3)−O(11)		92.4(2)
O(8)−Co(2)−O(5)		88.2(2)	O(9)−Co(3)−O(7)		83.3(2)
O(8[b])−Co(2)−O(5)		84.9(2)	O(14)−Co(3)−O(5)		95.3(2)
O(4)−Co(2)−O(5)		93.3(2)	O(11)−Co(3)−O(5)		115.3(2)
O(8[b])−Co(2)−O(13[a])		110.0(2)	Co(2)−O(5)−Co(3)		113.5(2)
O(4)−Co(2)−O(8)		178.2(2)	Co(2[a])−O(6)−Co(1)		101.0(2)
O(8)−Co(2)−O(6[a])		95.0(2)	Co(2[a])−O(13)−Co(1)		96.4(2)
O(8)−Co(2)−O(8[b])		83.2(2)	Co(2)−O(8)−Co(2[b])		96.8(2)

[a−f] Symmetry transformations used to generate equivalent atoms: $a = (-x, -y + 1, -z)$, $b = (-x - 1, -y, -z)$, $c = (-x - 2, -y, -z - 1)$, $d = (x - 1, y, z)$, $e = (x + 1, y + 1, z)$, and $f = (-x + 1, -y + 1, -z)$.

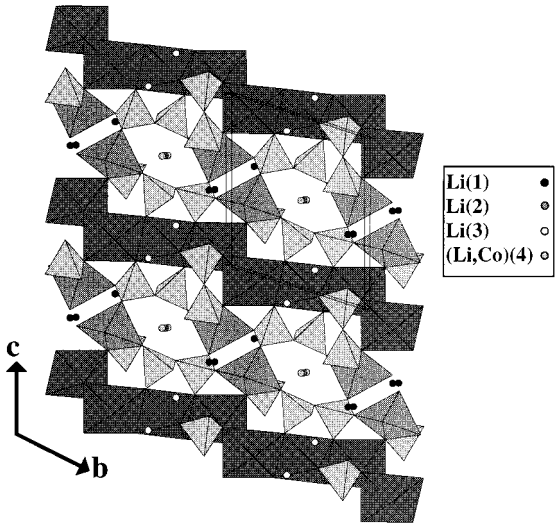

Figure 2. View of the $Li_6Co_5(P_2O_7)_4$ structure along [100], showing the A1 tunnels. Infinite $[Co_3O_{14}]_\infty$ chains in zigzag running along the *b* direction.

in the PO_4 tetrahedra and belong to the Li atoms coordination environment. The diphosphate group $P(2)P(4)O_7$ exhibits an almost eclipsed conformation with an angle P(2)−O(12)−P(4) of 138.5(3)° and the diphosphate $P(1)P(3)O_7$ exhibits an alternated conformation with an angle P(1)−O(2)−P(3) of 131.2(3)°. These angles are in the range of those found in other diphosphates.[5,9]

One of the main features in the structure of $Li_6Co_5(P_2O_7)_4$ involves the Li^+ environment in the tunnels. The maximum bond distance Li−O can determine the coordination number of Li^+ using the procedure by Donnay and Allmann[21] with the revised radii of Shannon[22] leading to 2.67 Å. In the title compound, there are four crystallographically independent Li atoms in the structure. Li(1) and Li(3) atoms are located at a (2i) general position and are surrounded by five oxygens, whereas Li(2) and Li,Co(4) are located at the (1h) and (1g) special positions and present octahedral coordination.

The CoO_6 polyhedra share edges forming infinite zigzag chains $[Co_3O_{14}]$ running along the *b* direction (Figure 2). In the *c* direction, such infinite chains share octahedra corners with CoO_5 polyhedra and P_2O_7 diphosphate groups doing the connection with another symmetrically equivalent chain. The connection between these chains defines tunnels, denoted as A1 hereafter, running along the *a* direction, and they are centered at $(x, {}^1/_2, {}^1/_2)$. These tunnels are delimited by six polyhedra (two CoO_5 trigonal bipyramids and four PO_4 tetrahedra) and present an hexagonal window. The Li(2) at $({}^1/_2, {}^1/_2, -{}^1/_2)$ and Li,Co(4) at $(0, {}^1/_2, -{}^1/_2)$ are located in these A1 tunnels, alternating between $x = {}^1/_2$ and $x = 0$.

In Figure 3, it can be observed that tunnels are formed in the [001] direction, labeled C1, and centered at $(0, {}^1/_2, z)$. As displayed, four octahedra and two tetrahedra are defining the C1 window. This figure shows the $[Co_3O_{14}]_\infty$ chains in zigzag running along *b*, the connection between them in the *a* direction is

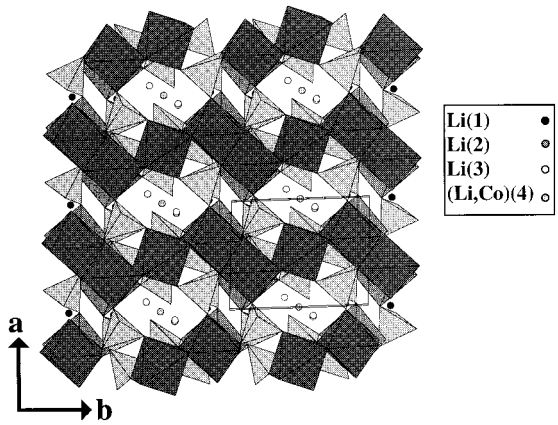

Figure 3. View of the $Li_6Co_5(P_2O_7)_4$ structure along [001], showing the C1 tunnels with the six-membered window.

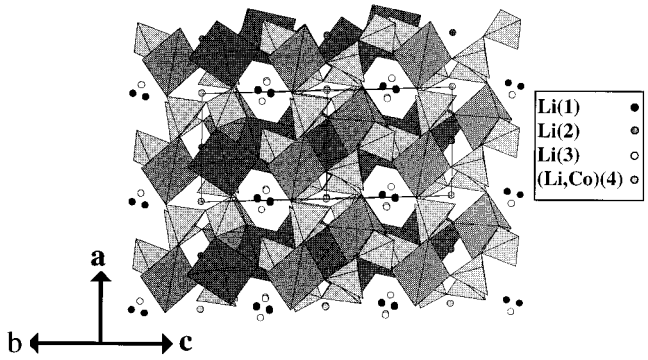

Figure 4. View of the $Li_6Co_5(P_2O_7)_4$ structure along [011], showing the D1 tunnels.

through the PO_4 groups. Li(3) and Li,Co(4) atoms are located in these C1 tunnels.

There are also channels along the [011] direction (Figure 4), denoted by D1, where Li(1), and Li(3) are located. These tunnels are delimited by six polyhedra (four CoO_6 octahedra, and two PO_4 tetrahedra).

The tunnel intersection gives rise to a three-dimensional channel system. The tunnels running along the [001] direction (C1) intersect those extending along the [100] direction (A1) (this situation can be denoted by A1 × C1). The intersection of the C1 and the D1 tunnels (C1 × D1) gives rise to the formation of a very open structure with a three-dimensional system of interconnecting channels. These tunnels, as we mentioned before, host the four crystallographically different lithium atoms. The Li(1) atoms are located inside D1 tunnels. Li(2) are located at A1 tunnels, and Li(3), and Li,Co(4) atoms lie at the interconnection of the tunnels (C1 × D1), and (A1 × C1), respectively.

Table 4 shows the cell parameters and distances range for the lithium transition-metal diphosphates structures known under our knowledge. Among the nine compounds, there are only seven different structural types. We are going to analyze here the differences and similarities between the title compound and others, giving a brief and clear description of the Li coordination in each one in order to contribute to a better insight into the crystal chemistry of the lithium transition-metal diphosphates.

In $Li_2MP_2O_7$ (M = Mo,[2] Fe,[3] V[4]), the structure consists of intersecting tunnels running along the [100] and ⟨110⟩ directions and the Li ions are located at the intersection

(20) Gillespie, R. J. *Molecular Geometry*; Van Nostrand Reynolds: London, 1972.
(21) Donnay, G.; Allmann, R. *Am. Mineral.* **1970**, *55*, 1003.
(22) Shannon, R. D. *Acta Crystallogr.* **1976**, *A32*, 751.

Table 4. Crystallographic Data for Lithium Transition-Metal Diphosphates

compound	*a* (Å), α	*b* (Å), *β*	*c* (Å), *γ*	*V* (Å^3)	SP	range (Li−O) (Å)	ref
$LiMP_2O_7$[a] M = Fe	4.8229(2)	8.0813(5), 109.387(5)°	6.9419(6)	255.2	$P2_1$	Fe = 1.99 (10)−2.14 (9) Mo = 1.969(3)−2.123(3) V = 1.960(10)−2.119(10)	3
$Li_2CuP_2O_7$	14.068(2)	4.8600(8), 98.97(1)°	8.604(1)	581.1	$I2/a$	1.87(1) − 1.94(1)	5
$Li_2PdP_2O_7$	12.5858(9)	7.4955(5)	5.8116(4)	548.2	$Imma$	2.003(3) − 2.452(4)	6
$LiMoOP_2O_7$	16.046(4)	11.951(2), 104.62(2)°	9.937(2)	1844.8(6)	$P2_1/n$	1.84(4) − 2.19(5)	7
$LiNi_{1.5}P_2O_7$	7.819(1)	7.744(2), 110.32(4)°	9.331(2)	487.2	$P2_1/c$	1.910(5) − 2.491(6)	8
$Li_6Co_5(P_2O_7)_4$	6.3009(7), 107.894(2)°	8.413(1), 90.247(2)°	9.937(1), 92.782(2)°	500.6	$P\bar{1}$	1.91(2) − 2.517(5)	[b]

[a] There are isostructural compounds when M = Mo[2] or V[4]. [b] Present paper.

of these tunnels and at the periphery. The Li ion is coordinated to four oxygen atoms at distances ranging from 1.93 to 2.14 Å, and the fifth neighboring oxygen atom is located at ≈2.65 Å. The large difference between the fifth bond and the other four suggests the lithium coordination as four. In the title compound, five oxygens surround Li(3), in the same way four shorter plus one longer (2.44(4) Å). The difference is not so large, but really if the longest Li(3)−O bond is eliminated, we may describe Li(3) as in tetrahedral coordination with an average Li(3)−O distance of 2.05(2) Å. Also in $LiNi_{1.5}P_2O_7$,[8] the Li polyhedron, we can find a gap between four O atoms, with distances range from 1.910(5) to 2.274(4) Å, and two others O atoms at larger distances, 2.491(6), and 2.703(4) Å. We can therefore consider that lithium has 5-fold rather than 6-fold coordination.

In $Li_2CuP_2O_7$[5] and $LiMoOP_2O_7$,[7] the Li cations are tetracoordinated in a distorted tetrahedral environment with Li−O distances ranging from 1.87(1) to 1.98(1) Å, and from 1.84(4) to 2.19(5) Å, respectively. The most interesting feature in $LiMoOP_2O_7$ deals with the fact that two LiO_4 tetrahedra share one edge, forming bitetrahedral units.

In the structure of $Li_2PdP_2O_7$,[6] due to the Pd square planar coordination, the LiO_6 octahedra play a very important role in order to ensure the three-dimensional character of the framework. LiO_6 octahedra share edges in such a way that they build infinite rutile chains running along the *c* direction. Two adjacent rows are connected by corners along *b*, leading to a layer. These layers, stacking in the *a* direction, are connected by diphosphate groups and PdO_4 square planes. The lithium atom exhibits a distorted octahedral environment, with two short bonds (2.003(3) Å), two long bonds (2.452(4) Å), and a Li−O average distance of 2.206 Å. If one considers only the four shortest distances, Li adopts a very distorted tetrahedral environment. In the title compound, Li(2) and Li,Co(4) are in octahedral coordination, Li,Co(4) with four short distances in square planar coordination and two longer (2.517(5) Å), and Li(2) with a Li−O average distance of 2.084(5) Å.

Magnetic Properties. In Figure 5a, the temperature dependence of the molar susceptibility χ and its reciprocal χ^{-1} for $Li_6Co_5(P_2O_7)_4$ are shown. At lower temperatures, the magnetic susceptibility rises to a maximum at 11 K. This behavior should be due to antiferromagnetic ordering of Co ions. In the range 70−300 K, the plot of χ^{-1} versus *T* can be fit to a Curie−Weiss law [$\chi^{-1} = 0.9(9) + 0.058(5)T$] ($r = 0.9999$) from which $C = 17.24$ cm^3 K/mol and $\theta = -16.9$ K were obtained. From the Curie constant, the effective magnetic moment per Co^{2+} ion, $\mu = 5.2\ \mu_B$ is obtained, which agrees with those reported for other Co(II) compounds.[23] It is worth nothing that the zero field splitting as well as the spin−orbit coupling would make significant contributions to the magnetic behavior of the title compound.[24]

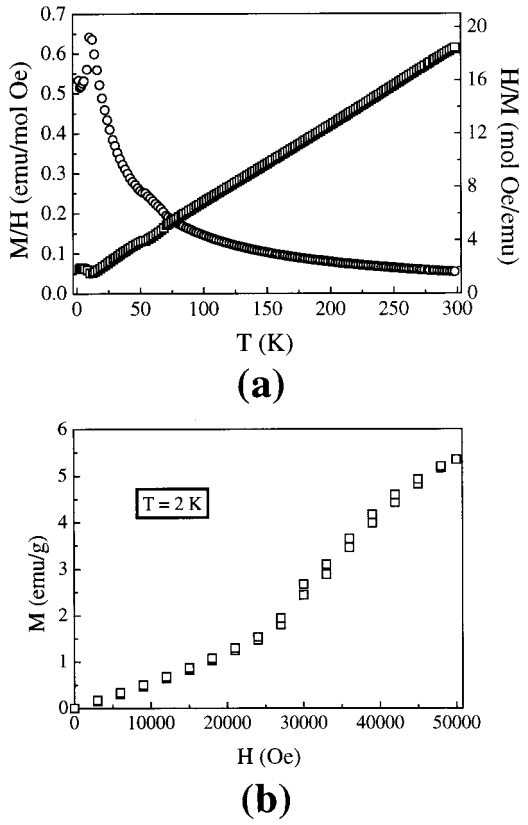

Figure 5. (a) Magnetic susceptibility (*M*/*H*, open circles) and inverse magnetic susceptibility (*H*/*M*, open squares) plotted as a function of temperature for $Li_6Co_5(P_2O_7)_4$. (b) *M* vs *H*, at 2 K, plots with the field increased and decreased.

The field dependence of magnetization is shown in Figure 5b. Because there is very little difference between 2 and 5 K data, only the field dependence data at 2 K are shown. The *M*(*H*) behavior shows that there is a metamagnetic transition at a critical field of about 24 000 Oe.

(23) Boudreaux, E. A.; Mulay, L. N. *Theory of Molecular Paramagnetism*; Wiley-Interscience Publication: New York, 1976.
(24) Zheng, L. M.; Lii, K. H. *J. Solid State Chem.* **1998**, *137*, 77.

By considering the structural features exhibited by this compound, different exchange pathways could be a priori involved in the observed magnetic behavior. The magnetic coupling between two adjacent metal centers in cobalt phosphates can be either through −O−P−O− bridges or −O− bridges.[25] The presence of Co−O−Co linkages has an important effect on the magnetic properties of this compound, and the most effective magnetic interactions occur through them. In $Li_6Co_5(P_2O_7)_4$, there are two different types of Co−O−Co bonds, one of them involves to the edge-sharing CoO_6 octahedra along the metal chains $(Co_3O_{14})_\infty$ and the other implicates the corner sharing between CoO_6 octahedra and CoO_5 trigonal bipyramids, as is shown in Figure 1. Therefore, an antiferromagnetic coupling between adjacent cobalt polyhedra is expected. Intermetallic angles are very different from 180° (Table 3), indicating a poor d-orbital overlapping.

On the other hand, the other exchange pathway implies the interaction through the P_2O_7 groups via Co−O−P−O−Co, leading to an antiferromagnetic three-dimensional magnetic behavior, as has been successful in other transition-metal phosphates.[26,27]

All of the discussed structural features justify the proposed antiferromagnetic ordering with an estimated Néel temperature as low as 11 K.

Acknowledgment. This work was supported by the Spanish CICYT and DGICYT under Project Nos. MAT98-0920, MAT98-1735, and PB97-1200. We thank Drs. A. Monge, R. Saez-Puche, and I. Rasines for fruitful comments.

Supporting Information Available: Structure factors, anisotropic displacement parameters, and bond lengths and angles for **1**. This material is available free of charge via the Internet at http://pubs.acs.org.

CM991085+

(25) Bu, X.; Feng, P.; Stucky, G. D. *J. Solid State Chem.* **1997**, *131*, 387.

(26) Forsyth, J. B.; Wilkinson, C.; Wanklyn, B. M. *J. Phys. Cond. Mater.* **1989**, *1*, 169.

(27) Goñi, A.; Lezama, L.; Barberis, G. E.; Pizarro, J. L.; Arriortua, M. I.; Rojo, T. *J. Magn. Magn. Mater.* **1996**, *164*, 251.